Hypercoordinated organotin compounds containing sulfur and chlorine. Molecular structures of $[(Ph_3P)_2N]^+[S(SnR_2Cl)_2Cl]^-$ (R = Me, t-Bu)

Jens Beckmann [a], Dainis Dakternieks [a,*], Andrew Duthie [a], Carissa Jones [a], Klaus Jurkschat [b], Edward R.T. Tiekink [c,d]

[a] *Centre for Chiral and Molecular Technologies, Deakin University, Geelong, Vic. 3217, Australia*
[b] *Fachbereich Chemie der Universität Dortmund, Lehrstuhl für Anorganische Chemie II, 44221 Dortmund, Germany*
[c] *Department of Chemistry, The University of Adelaide, Adelaide 5005, Australia*
[d] *Department of Chemistry, National University of Singapore, Singapore 117543*

Dedicated to Professor Oleg Nefedov on the occasion of his 70th birthday

Abstract

The reaction of diorganotin sulfides, $cyclo$-$(R_2SnS)_n$ (R = Me, n-Bu; $n = 3$; R = t-Bu; $n = 2$) with the corresponding diorganotin dichlorides, R_2SnCl_2, provided the tetraorganodistannathianes, $(R_2ClSn)_2S$ (**1**, R = Me; **2**, R = n-Bu; **3**, R = t-Bu). ^{1}H-, ^{13}C-, and ^{119}Sn-NMR studies indicate that these compounds are kinetically labile and in equilibrium with the starting materials. Addition of equimolar amounts of $[(Ph_3P)_2N]Cl$ to the reaction mixtures gave the chloride complexes $[(Ph_3P)_2N]^+[S(SnR_2Cl)_2Cl]^-$ (**4**, R = Me; **5**, R = n-Bu; **6**, R = t-Bu). Single-crystal X-ray diffraction studies revealed the tin atoms in both **4** and **6** to adopt distorted trigonal bipyramidal configurations with the chlorine atoms occupying the axial positions. © 2001 Elsevier Science B.V. All rights reserved.

Keywords: Hypercoordination; Organotin; Dimeric tin sulfides

1. Introduction

Dimeric tetraorganodistannoxanes $[R_2(X)SnOSn(Y)R_2]_2$ (X, Y = F, Cl, Br, OH, OR, OSiMe$_3$, OOCR, OSP(OR)$_2$, NO$_3$, N$_3$, NCS, SH, OReO$_3$; R = alkyl, aryl) have received great interest as catalysts for a variety of organic reactions. The catalytic activity has been attributed to the kinetic lability in solution of the ladder-like $Sn_4O_2X_2Y_2$ structural motif found in the solid state [1]. Dimeric tetraorganodistannoxanes $[R_2(X)SnOSn(X)R_2]_2$ (X = Cl, Br, OAc; R = alkyl) are easily accessible in high yields by reacting diorganotin oxides, R_2SnO, with diorganotin compounds, R_2SnX_2,

possessing two kinetically labile substituents X [2–4].

Some 30 years ago, Davies and Harrison [5] described the synthesis of analogous monomeric tetraorganodistannathianes $R_2(X)SnSSn(X)R_2$ (X = F, Cl, Br, I, SCN, OR, OOCR; R = alkyl) from the reaction of diorganotin sulfides, R_2SnS, with the appropriate diorganotin species, R_2SnX_2. However, the reported compounds were not well characterized at that time.

In the present work we briefly revisit the synthesis of tetraorganodistannathianes $R_2(Cl)SnSSn(Cl)R_2$ (R = Me, n-Bu, t-Bu) by the same method as reported by Davies and Harrison [5] and provide evidence that in some cases the products exist in equilibrium with the starting compounds. Repeating the same reaction in the presence of chloride ions gave rise to the formation of anionic sulfur- as well as chloride-bridged ditin complexes, namely $[S(SnR_2Cl)_2Cl]^-$ (R = Me, n-Bu, t-Bu), which were isolated as their $[(Ph_3P)_2N]^+$ salts.

* Corresponding author. Fax: + 61-3-5227-2218.
E-mail address: dainis@deakin.edu.au (D. Dakternieks).

2. Discussion

Reacting diorganotin sulfides, *cyclo*-(R$_2$SnS)$_n$ (R = Me, *n*-Bu, *t*-Bu; *n* = 2, 3), with the appropriate amounts of diorganotin dichlorides, R$_2$SnCl$_2$ (R = Me, *n*-Bu, *t*-Bu), in refluxing chloroform for 12 h resulted in clear solutions [5]. From these solutions, the solvents were allowed to evaporate slowly at room temperature leaving colorless microcrystalline (R = Me (**A**), R = *t*-Bu (**C**)) or waxy solids (R = *n*-Bu (**B**)). In contrast to the work of Davies and Harrison, we found that none of these solids gave sharp melting points but, instead, melt over wide temperature ranges [5]. This suggests that the solid materials **A**–**C** comprise a mixture of different compounds, presumably the starting compounds *cyclo*-(R$_2$SnS)$_n$ (*n* = 2, 3), and R$_2$SnCl$_2$ and/or the tetraorganodistannathianes R$_2$(Cl)SnSSn(Cl)R$_2$ (R = Me (**1**), *n*-Bu (**2**), *t*-Bu (**3**)).

The ^{119}Sn-NMR spectrum (CDCl$_3$) of material **A** shows a broad signal at 145.2 ppm revealing the presence of only one compound in solution, which is tentatively assigned to Me$_2$(Cl)SnSSn(Cl)Me$_2$ (**1**). In contrast to the dimeric structure of the corresponding tetraorganodistannoxane, [Me$_2$(Cl)SnOSn(Cl)Me$_2$]$_2$, the ^{119}Sn chemical shift suggests the tin atoms of **1** to be tetracoordinated. The ^{13}C- and ^{1}H-NMR spectra (CDCl$_3$) of **A** show a signal at 6.8 ppm ($^1J(^{13}$C–^{119}Sn) = 444 Hz) and 1.07 ppm ($^2J(^1$H–C–^{119}Sn) = 66 Hz), respectively.

For the material **B**, the ^{119}Sn-NMR spectrum (CDCl$_3$) reveals two broad signals in the tetracoordinated range at 136.5 (integral 85%) and 128.9 ppm (integral 15%), which are close to the chemical shifts reported for *cyclo*-(*n*-Bu$_2$SnS)$_3$ (δ 126.9) [6] and *n*-Bu$_2$SnCl$_2$ (δ 123.4) [7]. This observation is consistent with an equilibrium between *cyclo*-(*n*-Bu$_2$SnS)$_3$, *n*-Bu$_2$SnCl$_2$, and *n*-Bu$_2$(Cl)SnSSn(Cl)*n*-Bu$_2$ (**2**). Considering the very similar ^{119}Sn chemical shifts of the starting materials, no unambiguous assignment of the signals could be made. Apparently, the third signal is superimposed by one of the other broad signals. The ^{13}C-NMR spectrum (CDCl$_3$) of **B** shows a very broad signal at 29.1 ppm, two broad signals at 27.4 and 26.3 ppm and a reasonably sharp signal at 13.5 ppm. Consistent with this, the ^{1}H-NMR spectrum displays a broad signal at 1.73 ppm and two well-resolved multiplets at 1.37 and 0.92 ppm in an integral ratio of 4:2:3. The latter results suggest the assumed equilibrium between *cyclo*-(*n*-Bu$_2$SnS)$_3$, *n*-Bu$_2$SnCl$_2$, and *n*-Bu$_2$(Cl)SnSSn(Cl)*n*-Bu$_2$ (**2**) to be fast on the ^{1}H- and ^{13}C-NMR time scales.

The ^{119}Sn-NMR spectrum (CDCl$_3$) of the solid material **C** shows three distinctive signals at 125.5 ppm ($^2J(^{119}$Sn–S–^{117}Sn) = 117 Hz), 106.4 ($^2J(^{119}$Sn–S–^{117}Sn) = 160 Hz) and 55.0 ppm in an integral ratio of 1:1:1. The signals at 125.5 and 55.0 ppm are undisputedly correlated to the starting compounds *cyclo*-(*t*-

Bu$_2$SnS)$_2$ [8] and *t*-Bu$_2$SnCl$_2$ [6], respectively, while the signal at 106.4 ppm is unambiguously assigned to the tetraorganodistannathiane *t*-Bu$_2$(Cl)SnSSn(Cl)*t*-Bu$_2$ (**3**). The ^{13}C-NMR spectrum (CDCl$_3$) of material **C** exhibits two sets of signals, each consisting of three signals. The first set reveals signals belonging to the quaternary carbon atoms of the *tert*-butyl groups at 45.1 ($^1J(^{13}$C–^{119}Sn) = 395 Hz), 42.7 ($^1J(^{13}$C–^{119}Sn) = 330 Hz), and 39.3 ($^1J(^{13}$C–^{119}Sn) = 360 Hz) which are assigned to *t*-Bu$_2$SnCl$_2$, *t*-Bu$_2$(Cl)SnSSn(Cl)*t*-Bu$_2$ (**3**), and *cyclo*-(*t*-Bu$_2$SnS)$_2$, respectively. The second set shows signals at 30.0, 29.8 and 29.2 ppm, which are related to the methyl groups of the *tert*-butyl groups, however, no additional assignment was made for these signals. The ^{1}H-NMR spectrum (CDCl$_3$) of the solid material **C** also displays three equally intense signals at 1.44 ($^3J(^1$H–CC–$^{119/117}$Sn) = 114 Hz), 1.41 ($^3J(^1$H–CC–^{119}Sn) = 108 Hz), and 1.39 ppm ($^3J(^1$H–CC–$^{119/117}$Sn) = 90 Hz), which are assigned to *t*-Bu$_2$SnCl$_2$, *t*-Bu$_2$(Cl)SnSSn(Cl)*t*-Bu$_2$ (**3**), and *cyclo*-(*t*-Bu$_2$SnS)$_2$, respectively. The ^{119}Sn-, ^{13}C- and ^{1}H-NMR results are in agreement with an equilibrium between *cyclo*-(*t*-Bu$_2$SnS)$_2$, *t*-Bu$_2$SnCl$_2$, and *t*-Bu$_2$(Cl)SnSSn(Cl)*t*-Bu$_2$ (**3**) being slow on the NMR time scales.

In order to identify anionic organotin species associated with the aforementioned reactants in solution by autodissociation, electrospray mass spectra of acetonitrile solutions of **A**, **B** and **C** were recorded in the negative ion detection mode. In all cases the spectra revealed two intense mass clusters with distinctive isotope patterns related to the anions [R$_2$SnCl$_3$]$^-$ (254.9 for **A**, 338.9 for **B**, 338.9 for **C**) and [S(SnR$_2$Cl)$_2$Cl]$^-$ (436.8 for **A**, 605.0 for **B**, 605.0 for **C**). The detection of the latter anions supports the assignments made by NMR spectroscopy, and confirms the presence of tetraorganodistannathianes R$_2$(Cl)SnSSn(Cl)R$_2$ (R = Me (**1**), *n*-Bu (**2**), *t*-Bu (**3**)) in solutions of the materials **A**–**C**.

In summary, NMR spectroscopy and electrospray mass spectrometry reveal the existence of tetraorganodistannathianes in solutions of the materials **A**–**C**. The wide melting point ranges are consistent with a mixture of compounds in the solid state. Considering the kinetically labile Sn–Cl and Sn–S bonds, the most likely explanation for this observation is the assumption of equilibria between the starting materials and the tetraorganodistannathianes (Scheme 1).

Repeating the reaction of diorganotin sulfides, *cyclo*-(R$_2$SnS)$_n$ (R = Me, *n*-Bu, *t*-Bu; *n* = 2, 3), with the appropriate amounts of diorganotin dichlorides, R$_2$SnCl$_2$ (R = Me, *n*-Bu, *t*-Bu), in the presence of [(Ph$_3$P)$_2$N]Cl produced [(Ph$_3$P)$_2$N]$^+$[S(SnR$_2$Cl)$_2$Cl]$^-$ (R = Me (**4**), *n*-Bu (**5**), *t*-Bu (**6**)) in almost quantitative yields (Scheme 1). Notably, the organotin anions of compounds **4**–**6** resemble the electrospray mass clusters mentioned above. Compounds **4**–**6** represent colorless, sharp-melt-

ing crystalline solids that are highly soluble in common organic solvents.

The ^{119}Sn-NMR spectra (CDCl$_3$) of **4** and **5** show reasonably sharp signals in the range for pentacoordinated tin atoms at -32.3 and -35.3 ppm, respectively. The ^{13}C- and ^{1}H-NMR spectra (CDCl$_3$) are also consistent with the exclusive formation of **4** and **5** in solution (Section 3).

The ^{119}Sn-NMR spectrum (CDCl$_3$) of **6** reveals a sharp signal at 126.3 ppm ($^{2}J(^{119}$Sn$–$S$–^{117}$Sn$) = 119$ Hz, integral 37%), a broad signal at -2.3 ppm ($v_{1/2} = 200$ Hz, integral 40%) and a very broad signal at -18.3 ppm ($v_{1/2} = 400$ Hz, integral 23%), which are assigned
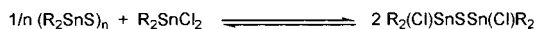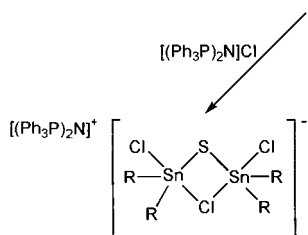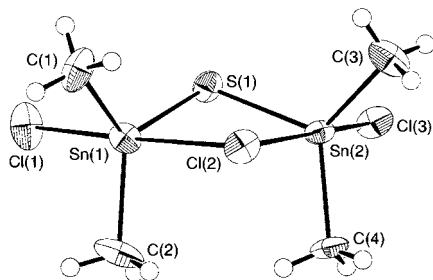
Scheme 1.

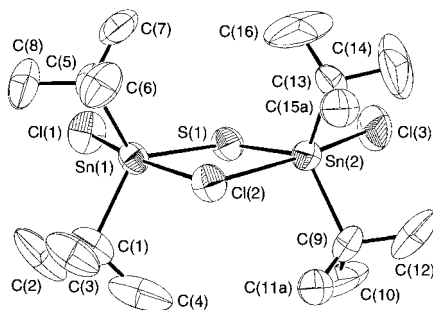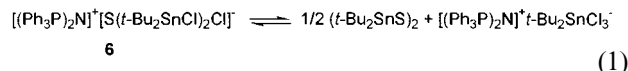Fig. 1. Molecular geometry for the anion in **4** showing the atomic numbering scheme.

Fig. 2. Molecular geometry for the anion in **6** showing the atomic numbering scheme. Only one component of each of the disordered C(11) and C(15) atoms is shown and hydrogen atoms have been omitted for clarity.

to *cyclo*-(t-Bu$_2$SnS)$_2$, t-Bu$_2$SnCl$_3^-$, and [S(Snt-Bu$_2$Cl)$_2$Cl]$^-$, respectively. Notably, the position of the signals associated with t-Bu$_2$SnCl$_3^-$ and [S(Snt-Bu$_2$Cl)$_2$Cl]$^-$ depend on the concentration of **6** in solution, however, no systematic studies were performed to account for this concentration dependence. The ^{13}C-NMR spectrum (CDCl$_3$) of **6** reveals two different sets of resonances, each containing three signals, in the range for alkyl carbon atoms. The signals related to the quaternary carbon atoms are centered at 45.9 ($^{1}J(^{13}$C$–^{119/117}$Sn$) = 674$ Hz), 41.2 ($^{1}J(^{13}$C$–^{119}$Sn$) = 459$ Hz), and 38.9 ppm ($^{1}J(^{13}$C$–^{119}$Sn$) = 356$ Hz), and were tentatively assigned to t-Bu$_2$SnCl$_3^-$, [S(Snt-Bu$_2$Cl)$_2$Cl]$^-$, and *cyclo*-(t-Bu$_2$SnS)$_2$, respectively. No assignment was made for the signals at 30.5, 29.6 and 29.3 ppm ascribed to the methyl groups of the *tert*-butyl groups. The ^{1}H-NMR spectrum (CDCl$_3$, low concentration) shows three signals in the range of the alkyl protons at 1.46 ($^{3}J(^{1}$H$–$CC$–^{119}$Sn$) = 118$ Hz, integral 45%), 1.43 ($^{3}J(^{1}$H$–$CC$–^{119}$Sn$) = 106$ Hz, integral 10%), and 1.40 ppm ($^{3}J(^{1}$H$–$CC$–^{119}$Sn$) = 96$ Hz, integral 45%), which are unambiguously assigned to t-Bu$_2$SnCl$_3^-$, [S(Snt-Bu$_2$Cl)$_2$Cl]$^-$, and *cyclo*-(t-Bu$_2$SnS)$_2$, respectively. Consequently, all NMR spectra of **6** are consistent with an equilibrium between [S(Snt-Bu$_2$Cl)$_2$Cl]$^-$, *cyclo*-(t-Bu$_2$SnS)$_2$ and t-Bu$_2$SnCl$_3^-$ in solution (Eq. (1)).

$$[(Ph_3P)_2N]^+[S(t\text{-}Bu_2SnCl)_2Cl]^- \rightleftharpoons 1/2\,(t\text{-}Bu_2SnS)_2 + [(Ph_3P)_2N]^+t\text{-}Bu_2SnCl_3^-$$
$$\mathbf{6}$$
$$\text{(1)}$$

2.1. Molecular structures of **4** and **6**

Precise structural information for **4** and **6** were afforded by single-crystal X-ray diffraction studies. The molecular structure of the anion in **4** is illustrated in Fig. 1, that for **6** in Fig. 2 and selected geometric parameters are collected in Table 1. The structures of **4** and **6** represent, as far as we are aware, the first crystallographically examples containing a Sn(μ-S)(μ-Cl)Sn core [9]. The anion in **4** is built up about a parallelogram defined by the aforementioned ditin core that has internal angles ranging from 82.50(5) to 100.22(7)°, with the most and least acute angles being subtended at the bridging Cl(2) and S(1) atoms, respectively. There is some disparity in the chloride bridge (ΔSn$–$Cl(2) is 0.08 Å) but the sulfide bridge is symmetrical. The coordination sphere of each of the tin atoms is completed by a terminal chlorine atom and two methyl groups. The geometry about each tin atom is best described as trigonal bipyramidal with the equatorial and axial positions being occupied by two C and one S, and by two Cl, respectively, in each case. The sum of the trigonal angles is 359.1(3) and 358.4(2)°, respectively, with the widest angle being subtended by the methyl substituents. In this description the Sn(1) atom

Table 1
Selected bond lengths (Å) and bond angles (°) for **4** and **6**

	4 [a]	**6** [b]
Sn(1)–S(1)	2.399(2)	2.380(2)
Sn(1)–Cl(1)	2.474(2)	2.513(3)
Sn(1)–Cl(2)	2.744(2)	2.743(3)
Sn(1)–C(1)	2.115(7)	2.17(1)
Sn(1)–C(x)	2.134(9)	2.179(10)
Sn(2)–S(1)	2.390(2)	2.388(3)
Sn(2)–Cl(2)	2.828(2)	2.755(2)
Sn(2)–Cl(3)	2.481(2)	2.482(2)
Sn(2)–C(y)	2.110(7)	2.18(1)
Sn(2)–C(z)	2.153(7)	2.19(1)
N(1)–P(1)	1.590(5)	1.558(7)
N(1)–P(2)	1.585(5)	1.539(7)
S(1)–Sn(1)–Cl(1)	89.41(6)	85.12(8)
S(1)–Sn(1)–Cl(2)	85.65(6)	81.44(8)
S(1)–Sn(1)–C(1)	117.8(2)	122.5(4)
S(1)–Sn(1)–C(x)	117.0(3)	119.0(3)
Cl(1)–Sn(1)–Cl(2)	175.06(6)	166.55(8)
Cl(1)–Sn(1)–C(1)	95.8(2)	96.9(3)
Cl(1)–Sn(1)–C(x)	93.7(3)	93.3(3)
Cl(2)–Sn(1)–C(1)	86.7(2)	90.0(3)
Cl(2)–Sn(1)–C(x)	88.4(3)	93.6(3)
C(1)–Sn(1)–C(x)	124.3(4)	118.2(4)
S(1)–Sn(2)–Cl(2)	83.98(6)	81.04(7)
S(1)–Sn(2)–Cl(3)	90.64(6)	84.60(9)
S(1)–Sn(2)–C(y)	116.8(2)	119.6(4)
S(1)–Sn(2)–C(z)	116.6(2)	120.5(3)
Cl(2)–Sn(2)–Cl(3)	173.63(6)	165.64(9)
Cl(2)–Sn(2)–C(y)	89.7(2)	92.4(3)
Cl(2)–Sn(2)–C(z)	83.6(2)	91.2(3)
C(y)–Sn–C(z)	125.0(3)	119.6(5)
Sn(1)–S(1)–Sn(2)	100.22(7)	108.11(9)
Sn(1)–Cl(2)–Sn(2)	82.50(5)	89.18(7)
P(1)–N(1)–P(2)	134.3(3)	145.0(5)

[a] $x = 2$, $y = 3$, $z = 4$.
[b] $x = 5$, $y = 9$, $z = 13$.

lies 0.1172(2) Å above the trigonal plane in the direction of the Cl(2) atom; the Sn(2) atom lies 0.1606(6) Å above its C_2S plane towards the Cl(3) atom. The respective Cl–Sn–Cl axial angles are 175.06(6) and 173.63(6)°. As expected, the Sn–Cl(bridging) distances are significantly longer than the Sn–Cl(terminal) distance. The closest contact in the lattice occurs between the ions such that Cl(1)···H(29)[i] is 2.66 Å; symmetry operation i: $2 - x$, $1/2 + y$, $-z$. The geometry of the $[(Ph_3)_2PN]^+$ cation is as expected [10]. The structure of the anion in **6** is in essential agreement with that found in **4** but with some notable differences.

The range of angles within the Sn(μ-S)(μ-Cl)Sn core is significantly greater in **6**, i.e. 81.04(7)–108.11(9)° and attendant with this is the observation that both chloride and sulfide bridges are symmetric. Clearly, there is a significant relief of steric strain within the Sn(μ-S)(μ-Cl)Sn core in **6** compared with that in **4** so that the angles subtended at the bridging S(1) and Cl(2) have increased by about 8 and 7°, respectively. This differ-

ence is also reflected in the planarity of the atoms comprising the core. Thus, in **6** the deviations of the Sn(1), Sn(2), S(1) and Cl(2) atoms from their least-squares plane are $-0.0031(6)$, $-0.0031(6)$, 0.088(3) and 0.062(3) Å, respectively. This contrasts the respective deviations of the atoms from the comparable plane in **4**, i.e. 0.0040(2), 0.0468(6), $-0.476(2)$, $-0.390(2)$ Å, indicating significant buckling. It would appear that this difference between the structures can be related to the substitution of the methyl groups in **4** by the *tert*-butyl groups in **6**.

An examination of the Sn-donor atom parameters listed in Table 1 reveals some interesting variations. The Sn(1)–Cl(2) distances are equivalent in **4** and **6** but, Sn(1)–S(1) and Sn(1)–Cl(1) are significantly shorter and longer, respectively, in **6**. Both pairs of Sn(2)–S(1) and Sn(2)–Cl(3) distances are experimentally equivalent in **4** and **6** but, Sn(2)–Cl(2) is significantly shorter in **6**. A consistent observation is that the magnitude of the Sn–C bond distances are increased in **6** compared with **4**. With the exception of the narrowing of the C–Sn–C angles (by ca. 5°) in **6** compared with those in **4**, the majority of angles subtended at the tin atoms involving a carbon atom in **6** are either equivalent (one case) or significantly wider. Notably, this has the result that the S–Sn–Cl and Cl–Sn–Cl angles are uniformly more acute in **6**. The reduction in these latter angles is accompanied by an expansion of the Sn(1)–S(1)–Sn(2) and Sn(1)–Cl(2)–Sn(1) angles and hence, a reduction of steric strain at the bridging atoms.

The ^{119}Sn-MASNMR spectrum of **6** reveals two signals at -75.8 and -82.5 ppm, and is therefore fully consistent with the number of crystallographically independent tin sites in the molecular structure. The closest non-hydrogen (and non-disordered component) contact in the lattice occurs between the C(7) and C(32)[ii] atoms, i.e. between anion and cation, at 3.51(2) Å; symmetry operation ii: x, $1 - y$, $3/2 - z$.

3. Experimental

All manipulations with air sensitive compounds were carried out under Ar using standard vacuum line and Schlenk techniques. Reagent grade solvents were dried over the appropriate desiccants and freshly distilled prior to use. *cyclo*-$(Me_2SnS)_3$, *cyclo*-$(n$-$Bu_2SnS)_3$, [11] *cyclo*-$(t$-$Bu_2SnS)_2$, [8] and t-Bu_2SnCl_2 [12] were prepared according to literature procedures. Me_2SnCl_2, n-Bu_2SnCl_2, and $[(Ph_3P)_2N]Cl$ were obtained from Fluka and Aldrich. NMR spectra were recorded using a Varian 300 MHz Unity Plus NMR spectrometer. ^{1}H, ^{13}C, ^{31}P and ^{119}Sn chemical shifts (δ) are given in ppm and are referenced against Me_4Si, H_3PO_4, and Me_4Sn. Electrospray mass spectra were obtained with a Platform II single quadrupole mass spectrometer (Micro-

mass, Altrincham, UK) using an MeCN mobile phase. Acetonitrile solutions (0.1 mM) of the compounds were injected directly into the spectrometer via a Rheodyne injector equipped with a 50 μl loop. A Harvard 22 syringe pump delivered the solutions to the vaporization nozzle of the electrospray ion source at a flow rate of 10 μl min^{-1}. Nitrogen was used as both a drying gas and for nebulization with flow rates of ca. 200 and 20 ml min^{-1}, respectively. Pressure in the mass analyzer region was usually about 4×10^{-5} mbar. Typically ten signal-averaged spectra were collected. Microanalyses were performed by CMAS, Belmont, Australia.

3.1. Reactions between cyclo-(R$_2$SnS)$_n$ and R$_2$SnCl$_2$ (R = Me, n-Bu, t-Bu; n = 2, 3)

A mixture of *cyclo*-(R$_2$SnS)$_n$ (181 mg, 0.33 mmol for R = Me, n = 3; 265 mg, 0.33 mmol for R = n-Bu, n = 3, 265 g, 0.50 mmol for R = t-Bu, n = 2) and R$_2$SnCl$_2$ (219 mg, 1.00 mmol for Me; 304 mg, 1.00 mmol for R = n-Bu; 304 g, 1.00 mmol for R = t-Bu) in CHCl$_3$ (3 ml) was heated at reflux for 12 h. The solvent was allowed to evaporate slowly to give microcrystalline or waxy solid materials, designated as **A** (R = Me, m.p. 55–164 °C), **B** (R = n-Bu, m.p. 36–44 °C), and **C** (R = t-Bu, m.p. 61–145 °C). ^{119}Sn-, ^{13}C- and ^{1}H-NMR spectra were discussed in the text.

3.2. Synthesis of [(Ph$_3$P)$_2$N]$^+$[S(SnR$_2$Cl)$_2$Cl]$^-$ (R = Me (4), n-Bu (5), t-Bu (6))

A mixture of *cyclo*-(R$_2$SnS)$_n$ (181 g, 0.33 mmol for R = Me, n = 3; 265 g, 0.33 mmol for R = n-Bu, n = 3; 265 g, 0.50 mmol for R = t-Bu, n = 2), R$_2$SnCl$_2$ (219 mg, 1.00 mmol for Me; 304 mg, 1.00 mmol for R = n-Bu; 304 g, 1.00 mmol for R = t-Bu), and [(Ph$_3$P)$_2$N]Cl (574 mg, 1.00 mmol) in CHCl$_3$ (3 ml) was heated at reflux for 12 h. The solvent was removed in vacuo to give colorless crystalline materials, which were recrystallized from hexane–CH$_2$Cl$_2$.

[(Ph$_3$P)$_2$N]$^+$[S(SnMe$_2$Cl)$_2$Cl]$^-$ (**4**) (926 mg, 95%, m.p. 194–195 °C). ^{1}H-NMR (CDCl$_3$): $\delta = 7.7$–7.4 (m, 30H; *Ph*), 1.14 (s, 12H, $^{1}J(^{1}H$–$^{119/117}$Sn) = 76 Hz; *Me*). ^{13}C-NMR (CDCl$_3$): $\delta = 133.7$, 131.8, 129.4, 126.6 (*phenyl carbons*), 13.0 ($^{1}J(^{13}C$–^{119}Sn) = 573 Hz; *Me*). ^{31}P-NMR (CDCl$_3$): $\delta = 21.2$. ^{119}Sn-NMR (CDCl$_3$): $\delta = -34.3$. Anal. Found. C, 49.2; H, 4.2; Cl, 10.9; N, 1.3. Calc. for C$_{40}$H$_{42}$Cl$_3$NP$_2$SSn$_2$ (974.6): C, 49.3; H, 4.3; N, 1.4; Cl, 10.9%.

[(Ph$_3$P)$_2$N]$^+$[S(Snn-Bu$_2$Cl)$_2$Cl]$^-$ (**5**) (982 mg, 86%, m.p. 97–99 °C). ^{1}H-NMR (CDCl$_3$): $\delta = 7.7$–7.4 (m, 30H; *Ph*), 1.83 (tt, 8H; SnCH$_2$CH_2), 1.67 (t, 8H, $^{2}J(^{1}H$–C–$^{119/117}$Sn) = 72 Hz; SnCH_2), 1.38 (tq, 8H; CH_2CH$_3$), 0.88 (t, 12H; CH$_2$CH_3). ^{13}C-NMR (CDCl$_3$): $\delta = 133.7$, 131.8, 129.4, 126.6 (*phenyl carbons*), 31.4

($^{1}J(^{13}C$–^{119}Sn) = 535 Hz), 27.8 ($^{2}J(^{13}C$–C–$^{119/117}$Sn) = 34 Hz), 26.2 ($^{3}J(^{13}C$–CC–$^{119/117}$Sn) = 102 Hz), 13.6. ^{31}P-NMR (CDCl$_3$): $\delta = 21.2$. ^{119}Sn-NMR (CDCl$_3$): $\delta = -35.3$. Anal. Found. C, 55.4; H, 6.3; Cl, 9.6; N, 1.2. Calc. for C$_{52}$H$_{66}$Cl$_3$NP$_2$SSn$_2$ (1143.0): C, 54.7; H, 5.8; Cl, 9.3; N, 1.2%.

[(Ph$_3$P)$_2$N]$^+$[S(Snt-Bu$_2$Cl)$_2$Cl]$^-$ (**6**) (1052 mg, 92%, m.p. 193–194 °C). ^{1}H-NMR (CDCl$_3$): $\delta = 1.46$ ($^{3}J(^{1}H$–CC–^{119}Sn) = 118 Hz, integral 45%; *t*-Bu$_2$SnCl$_3^-$), 1.43 ($^{3}J(^{1}H$–CC–^{119}Sn) = 106 Hz, integral 10%; **6**), 1.40 ($^{3}J(^{1}H$–CC–^{119}Sn) = 96 Hz, integral 45%; *cyclo*-(*t*-Bu$_2$SnS)$_2$). ^{1}H-NMR (CDCl$_3$): $\delta = 133.7$, 131.8, 129.4, 126.6 (PPN), 45.9 ($^{1}J(^{13}C$–$^{119/117}$Sn) = 674 Hz; C*Me*$_3$, *t*-Bu$_2$SnCl$_3^-$), 41.2 ($^{1}J(^{13}C$–^{119}Sn) = 459 Hz; C*Me*$_3$, **6**), 38.9 ($^{1}J(^{13}C$–^{119}Sn) = 356 Hz; C*Me*$_3$, *cyclo*-(*t*-Bu$_2$SnS)$_2$), 30.5, 29.6, 29.3 (C*Me*$_3$). ^{31}P-NMR (CDCl$_3$): $\delta = 21.1$. ^{119}Sn-NMR (CDCl$_3$): $\delta = 126.3$ ($^{2}J(^{119}$Sn–S–^{117}Sn) = 119 Hz, integral 37%; *cyclo*-(*t*-Bu$_2$SnS)$_2$), -2.3 (integral 40%, *t*-Bu$_2$SnCl$_3^-$), -18.3 (integral 23%, **6**). ^{119}Sn-MAS NMR: $\delta = -75.8$, -82.5. Anal. Found. C, 54.8; H, 6.0; Cl, 9.3; N, 1.2. Calc. for C$_{52}$H$_{66}$Cl$_3$NP$_2$SSn$_2$ (1143.0): C, 54.7; H, 5.8; Cl, 9.3; N, 1.2%.

3.3. Crystallography

Intensity data for colorless **4** and **6** were measured on a Rigaku AFC7R (AFC6R for **6**) diffractometer at 173 K (293 K for **6**) employing Mo–K$_\alpha$ radiation and the ω:2θ scan technique such that $\theta_{\max}$ was 27.5° (27.9°). Corrections were made for Lorentz and polarization effects [13] and for absorption employing an empirical procedure [14]. Crystallographic data are summarized in Table 2.

Each structure was solved by heavy-atom methods [15] and refined by a full-matrix least-squares procedure based on F [13]. For **4**, non-hydrogen atoms were refined with anisotropic displacement parameters and hydrogen atoms were included in the model at their calculated positions. An analogous strategy was employed in the refinement of **6** with the following exception. Significant thermal motion was noted for the methyl groups and for two of these, i.e. the C(11) and C(15) atoms, two distinct positions were discerned. From isotropic refinement, these were ascribed 50% site occupancy factors; hydrogen atoms were not included for the disordered groups. After the inclusion of a weighting scheme of the form $w = 1/[\sigma^2(F) + g|F|^2]$, the refinements were continued until convergence. The absolute structure of **4** was determined based on differences in the refinements for the opposite hands. Final refinement details are given in Table 2 and the crystallographic numbering schemes are shown in Figs. 1 and 2 which were drawn at the 50% probability level [16].

Table 2
Crystallographic data and structural parameters for **4** and **6**

Compound	4	6
Empirical formula	$C_{40}H_{42}Cl_3NP_2SSn_2$	$C_{52}H_{66}Cl_3NP_2SSn_2$
Formula weight	974.5	1142.9
Crystal size (mm)	$0.11 \times 0.21 \times 0.57$	$0.07 \times 0.11 \times 0.36$
Crystal system	Monoclinic	Monoclinic
Space group	$P2_1$	$C2/c$
Unit cell dimensions		
a (Å)	10.886(4)	39.75(1)
b (Å)	12.662(6)	14.872(4)
c (Å)	14.925(3)	19.983(6)
β (°)	92.63(2)	112.39(3)
V (Å^3)	2055(1)	10921(6)
Z	2	8
D_{calc} (cm^{-3})	1.575	1.390
$F(000)$	972	4656
μ (cm^{-1})	15.68	11.91
Measured data	5196	11564
Unique data	4946	11372
Data with $I \geq n\sigma(I)$	3799, $n = 3$	4722, $n = 2$
R	0.028	0.054
g	0.004	0.00001
R_w	0.028	0.040
ρ (e Å^{-3})	0.39	0.64

4. Supplementary material

Crystallographic data for the structural analysis have been deposited with the Cambridge Crystallographic Data Centre, CCDC nos. 160108 and 157770 for compounds **4** and **6**, respectively. Copies of this information may be obtained free of charge from The Director, CCDC, 12 Union Road, Cambridge CB2 1EZ, UK (Fax: +44-1223-336033; e-mail: deposit@ccdc.cam.ac.uk or www: http://www.ccdc.cam.ac.uk).

References

[1] J. Beckmann, K. Jurkschat, U. Kaltenbrunner, S. Rabe, M. Schürmann, D. Dakternieks, A. Duthie, D. Müller, Organometallics 19 (2000) 4887 (and references cited therein).
[2] A.G. Davies, P.G. Harrison, P.R. Palan, J. Chem. Soc. C (1970) 2030.
[3] D. Dakternieks, K. Jurkschat, S. van Dreumel, E.R.T. Tiekink, Inorg. Chem. 36 (1997) 2023.
[4] J. Beckmann, K. Jurkschat, S. Rabe, M. Schürmann, D. Dakternieks, Z. Anorg. Allg. Chem. 627 (2001) 458.
[5] A.G. Davies, P.G. Harrison, J. Chem. Soc. C (1970) 2035.
[6] B. Wrackmeyer, Annu. Rep. NMR Spectrosc. 16 (1985) 73.
[7] P.J. Smith, L. Smith, Inorg. Chim. Acta Rev. 7 (1973) 11.
[8] H. Puff, G. Bertram, B. Ebeling, M. Franken, R. Gattermayer, R. Hundt, W. Schuh, R. Zimmer, J. Organomet. Chem. 379 (1989) 235.
[9] G.R. Lewis, I. Dance, J. Chem. Soc. Dalton Trans. (2000) 299.
[10] F.H. Allen, O. Kennard, Chem. Des. Automat. News (1993) 8.
[11] H. Schumann, Z. Anorg. Allg. Chem. 354 (1967) 192.
[12] A.L. Allred, S.A. Kandil, J. Chem. Soc. A (1970) 2987.
[13] TEXSAN, Structure Analysis Package, Molecular Structure Corporation, TX, 1992.
[14] N. Walker, D. Stuart, Acta Crystallogr. Sect. A 39 (1983) 158.
[15] P.T. Beurskens, G. Admiraal, G. Beurskens, W.P. Bosman, S. García-Granda, J.M.M. Smits, C. Smykalla, The DIRDIF Program System, Technical Report of the Crystallography Laboratory, University of Nijmegen, The Netherlands, 1994.
[16] C.K. Johnson, ORTEP-II, Report ORNL-5138, Oak Ridge National Laboratory, Oak Ridge, TN, 1976.